Supplementary matierials

Supplementary Methods

MRI scan and hippocampal examination

A 3.0 T MRI scanner with a standard 8-channel head coil was used. T1 FLAIR, T2 FLAIR, T2WI, sagittal T2FSE, and DWI images were obtained to exclude irrelevant intracranial lesions (T1FLAIR: TR=2000 ms, TE=24 ms, FOV=240×240 mm, slice thickness=4 mm, slice interval=1 mm; T2FLAIR: TR=8000 ms, TE=155 ms, TI=2100 ms, FOV=240×240 mm, slice thickness=4 mm, slice interval=1 mm; T2WI: TR=4600 ms, TE=106 ms, FOV=240×240 mm, slice thickness=4 mm, slice interval=1 mm; T2FSE(sagittal): TR=4500 ms, TE=120 ms, FOV=240×240 mm, slice thickness=4 mm, slice interval=1 mm. DWI: TR=5200 ms, TE=74 ms, FOV=240×240 mm, slice thickness=4 mm, slice interval=1 mm). The double-location method was employed to locate the optimum sagittal plane of the hippocampus. The line was positioned vertical to the long axis of the hippocampus. The angle was adjusted according to the transection plane to ensure that the line was vertical relative to the midline of the brain. Images of the oblique-axial and oblique-coronal planes of the hippocampus were obtained. The scanning parameters were set as follows: T2; TR=4200 ms, TE=121 ms, FOV=240×240 mm, slice thickness=4 mm, slice interval=1 mm. The medial temporal atrophy (MTA) scale was adopted to evaluate the degree of hippocampal atrophy as previous papers (Scheltens, 1992). MTA scores were independently determined by a neurologist and a radiologist based on previous studies. Any discrepancy was resolved by discussion. Abnormal outcomes were defined as follows: MTA score ≥1 in patients aged <65 years, MTA score ≥2 in patients aged 66-75 years, and MTA score ≥3 in patients aged ≥75 years. The MTA method only provides a rough evaluation of hippocampal atrophy, although it is included in the diagnostic criteria of the National Institute on Ageing-Alzheimer's Association (NIA-AA) for Alzheimer's disease and mild cognitive impairment. The current NIA-AA guidelines do not specify the specific method of MTA measurement.

In the current study, we measured the hippocampus head and main body (Figure 1A), where the most significant atrophy was observed. The width of the temporal horn of the hippocampus was also determined to assess the degree of hippocampal atrophy. The measurement was separately performed by 2 radiologists and finally the mean value were obtained to exclude possible errors. All data from the patients subject to random sampling inspection by a third person. The error rate of input data should be lower than 0.5%.

Blood sampling

Peripheral blood (4 ml) was sampled and centrifuged at 300 g for 5 min at 4 °C. One milliliter of whole blood was used for APOE genotyping, and 3 ml whole blood was used for the collection of plasma and PBMC. The supernatant (plasma) was collected for a subsequent examination of the levels of inflammatory factors. The peripheral blood mononuclear cells (PBMCs) were isolated using the Histopaque density gradient method for RNA sequencing (the details are displayed in the Supplementary Materials).

***APOE* genotyping**

APOE genotyping was performed using the SNaPshot Multiplex System as described in a previous paper. By sequencing rs429358 and rs7412 in exon 4 of the *APOE* gene, the *APOE* status was defined as the presence of one or more copies of *E2*, *E3*, and *E4*. An *APOE* ε4-positive status was confirmed as the ε4/ε4, ε3/ε4, or ε2/ε4 genotype, whereas the other genotypes were defined as non-APOE4 carriers (Wei and Chen, 2021).

Inflammatory cytokine measurements using Luminex liquid chip technology

In this study, Luminex liquid chip technology was used to detect the plasma levels of 13 inflammatory cytokines, as follows, in patients with AD: TNF-α, IFN-γ, IL-1β, IL-5, IL-6, IL-7, IL-8, IL-10, IL-13, IL-17, IL-18, IL-33, and MCP-1. The specific method is to establish gradient 3-fold dilutions of the standard to set seven concentration gradients. Blood samples and the standard were added to 96-well plates, and then a mixture of 500 μl of premixed magnetic beads and 5 ml of RD2-1 was

added. The 96-well plate was placed on the magnetic plate and incubated for 2 min before it was inverted on a paper towel to remove the liquid from each well, and then cleaning solution was added once. Fifty microliters of antibody were added to the corresponding well, the plate was covered with transparent film, and the plate was incubated on an 800 rpm shaking table for 2 h. After shaking and washing the plate, 50 μl of detection antibody was added, and the plate was incubated on an 800 rpm shaking table for 1 h. After shaking and washing the plate, 50 μl of SA-PE were added. After coating, the plate was shaken and incubated on an 800 rpm shaking table for 30 min. The plate was read using the Luminex 200 instrument after washing with the following parameters: DD gate, 8000-20000; timeout, 60 s; and bead event, 50.

Measurement of plasma Aβ levels

Plasma Aβ1-42 and Aβ1-40 levels were detected using liquid phase flow cytometry (using the MSD platform) to evaluate the outcomes of pathological indicators (Wei and Chen, 2021).

Bulk RNA-sequencing and analysis of PBMC

RNA was extracted from PBMCs in 10 patients with AD (four non-*APOE4* carriers and six *APOE4* carriers) using standard extraction methods. RNA samples were then subjected to quality control using agarose gel electrophoresis,Agilent 2100 bioanalyzer, and NanoPhotometer spectrophotometer. Bulk RNA-seq libraries were prepared using NEBNext® Ultra™ RNA Library Prep Kit for Illumina®. Using fragmented mRNA as templates and random oligonucleotides as primers, the first strand of cDNA was synthesized in the Moloney Murine Leukemia Virus (M-MuLV, MMLV) Reverse Transcriptase system, and then the RNA strand was degraded with RNase H. The second strand of cDNA was synthesized using dNTPs in the DNA polymerase I system. The purified double-stranded cDNA was end-repaired, A-tailed. The adapters were ligated to the DNA fragments. After the cDNA screening by AMPure XP beads and PCR amplification, the Illumina sequencing was performed. The differential expression genes were imported into Metascape (http://metascape.org/) for gene ontology analysis of biological processes and the

Kyoto Encyclopedia of Genes and Genomes (KEGG), and WikiPathways analysis was performed with a false discovery rate (FDR) <0.01 as the cut-off value.

Single-cell sequencing and analysis of PBMC

Sample pooling strategies were used in four non-carrier PBMC and six carrier PBMC. Single-cell RNA-Seq libraries were prepared using the SeekOne® MM Single Cell 3' library preparation kit, and then sequenced on illumina NovaSeq 6000 with PE150 read length or DNBSEQ-T7 platform with PE100 read length. Single cell RNA-seq cell ranger pipeline and cell clusters analysis, single cell RNA-seq functional and pathway enrichment analysis, and single cell RNA-seq protein–protein interaction network analysis were performed. Briefly, appropriate number of cells were loaded into the flow channel of SeekOne® MM chip, which had 170,000 microwells, and allowed to settle in microwells by gravity. After removing the unsettled cells, sufficient Cell Barcoded Magnetic Beads (CBBs) were pipetted into flow channel and also allowed to settle in microwells with the help of a magnetic field. Next, excess CBBs were rinsed out and cells in MM chip were lysed to release RNA which was captured by the CBB in the same microwell. Then, all CBBs were collected and reverse transcription were performed at 37 ℃ for 30 min to label cDNA with cell barcode on the beads. Further Exonuclease I treatment were performed to remove unused primer on CBBs. Subsequently, barcoded cDNA on the CBBs was hybridized with random primer which had reads 2 SeqPrimer sequence on the 5' end and could extend to form the second strand DNA with cell barcode on the 3' end. The resulting second strand DNA was denatured off the CBBs, and purified and amplified in a PCR reaction. The amplified cDNA product was then cleaned to remove unwanted fragment and added to full length sequencing adapter, and sample index was generated by indexed PCR. The indexed sequencing libraries were cleaned up with SPRI beads, quantified by quantitative PCR (KAPA Biosystems KK4824), and sequenced on illumina NovaSeq 6000 with PE150 read length or DNBSEQ-T7 platform with PE100 read length.

Single cell RNA-seq cell ranger pipeline and cell clusters analysis

The Cell Ranger software (10X Genomics) obtained from https://support.10xgenomics.com/single-cell-gene-expression/software/downloads/latest was used to perform barcode and unique molecular identifier counting after filtering and alignment to the GRCh37 (hg19) reference genome to generate the feature-barcode matrix and determine clusters. Dimensionality reduction was performed using principal component analysis, and the first ten principal components were used to generate clusters by the K means and graph-based algorithms, respectively. Data analysis was performed through the Loupe Cell Browser software (10X Genomics) on Cloupe files displaying UMAP (Uniform Manifold Approximation and Projection) projections of cell transcriptome.

Single cell RNA-seq functional and pathway enrichment analysis

The differential expression genes for each cell type were imported into Metascape (http://metascape.org/) for gene ontology analysis of biological processes and the Kyoto Encyclopedia of Genes and Genomes (KEGG). WikiPathways analysis was performed with a false discovery rate (FDR) <0.01 as the cut-off value.

Single cell RNA-seq protein–protein interaction network analysis

Protein–protein interaction network analysis (PPI) was performed using Metascape. The molecular complex detection (MCODE) algorithm was used to identify closely related modules in the network.

Cell-cell interaction analysis

The R-package CellChat (v 1.1.3) was used to infer cell-cell interaction networks.

Statistical Analysis

The data are presented as the means ± SD. All data were analyzed using the SPSS version 22 (IBM) software, and the P-value for the comparison between groups was considered statistically significant at less than 0.05. Differences in age, education level, neuropsychological assessment, plasma amyloid-β peptide levels, plasma levels of inflammatory cytokines, and hippocampal height between *APOE4* carriers and non-carriers were compared using independent-samples t-test or Mann–Whitney test. Differences in sex and comorbidities were compared using the chi-square test.

Pearson's linear correlation coefficients were calculated to analyze the correlations between hippocampal height and plasma levels of inflammatory cytokines or amyloid β peptides. Linear regression analysis was also used to compare correlations between hippocampal height and plasma levels of inflammatory cytokines.

The Expression of *E3*，*E4* in SY5Y

In order to investigate differences in the expression of IL-7R pathways betwen *APOE4* carrier and non-carrier, we used SY5Y cells overexpressing *APOE3* or *APOE4* to detect the differences (SH-SY5Y-hAPOE3-3flag-ZsGreen-Puro and SH-SY5Y-hAPOE4-3flag-ZsGreen-Puro). Successful expression was verified by polymerase chain reaction (PCR) and gene sequencing. The primer of *APOE* used for PCR amplification were:

hAPOE-EcoRI-F

5:-CCGGAATTCGCCACCATGAAGGTTCTGTGGGCTGCGTTGCT-3'

hAPOE-SpeI-R:

5:'-CTAGACTAGTGTGATTGTCGCTGGGCACAGGGGCGG-3'

The SY5Ys were cultured in single-cell configuration onto 6-well plates before lentiviral transfection. Then, 30 μl lentivirus (10^9/ml) was added to each well (multiplicity of infection [MOI] approx. 50:1). After overnight incubation, the medium was replaced. Cells that were not transfected after 3 days were screened with puromycin antibiotics, and the medium was replaced after 3 days. Fluorescence photography was performed after the medium was changed.

QPCR

After collecting from 6-well plates, the total RNA of *APOE3* and *APOE4* were extracted following the manufacturer's protocols. A spectrophotometer at 260/280 nm was used to measure RNA concentrations and purity, and samples with absorbance ratios between 1.8-2.1 were considered acceptable. Using a PrimeScrip RT Master Mix, complementary DNA was synthesized from total RNA. Melting curves were generated after PCR to identify sequence-specific products.Using a melting curve

program and continuous fluorescence measurements, melting curve analysis was carried out. Two-fold data conversions were applied to quantify relative gene expression and normalized to GAPDH. Six biological replicates with three technical replicates were used for each PCR assay.

IL7R_F	CCCTCGTGGAGGTAAAGTGC
IL7R_R	CCTTCCCGATAGACGACACTC
CD28_F	CTATTTCCCGGACCTTCTAAGCC
CD28_R	GCGGGGAGTCATGTTCATGTA
JUN_F	TCCAAGTGCCGAAAAAGGAAG
JUN_R	CGAGTTCTGAGCTTTCAAGGT
ULBP2_F	GTTCAAGGCCAGGTGGATGA
ULBP2_R	GGGACTGACAGGTGTGACTG

Supplementary results

***APOE*4 allele decreased the expression of IL7R and CD28 in SY5Y cells.**

To verify the effect of *APOE4* allele on IL-7 receptor expression, we used lentiviral transfection to overexpress *APOE3* or *APOE4* in SY5Y cells, respectively. Under fluorescence microscopy, both overexpressing *E3* and *E4* showed very high expression efficiency (*Supplementary Figure 2A*). We used qPCR to detect the expression of genes such as IL-7R, CD28, ULBP2, JUN, etc. The results showed that SY5Y cells had lower expression of IL7R, CD28, and ULBP2. However, compared to *APOE3* cells, overexpressing the *APOE4* allele showed a significant trend of low expression in IL7R and CD28 (*Supplementary Figure 2B*).

Supplementary Figure legends

Supplementary Figure 1| Correlations Between Inflammatory Cytokines, Cognitive Measures, Amyloid Levels, and Hippocampal Atrophy in Patients. **(A)**.This sub-figure illustrates the correlations between various inflammatory cytokine levels, cognitive assessments (MMSE and MoCA), Aβ1-40, Aβ1-42, Aβ1-42/Aβ levels, and the extent

of atrophy in the left hippocampus among individuals who are non-*APOE4* carriers. These correlation analyses provide insights into the relationships among these factors and their potential impact on left hippocampal atrophy in this subgroup. **(B)**.In a similar context, this sub-figure depicts the correlations between inflammatory cytokine levels, cognitive assessments, amyloid levels, and the degree of atrophy in the right hippocampus for non-*APOE4* carriers. It offers a view of how these variables are interrelated and their potential influence on right hippocampal atrophy within this group. **(C)**.Shifting the focus to *APOE4* carriers, this sub-figure showcases the correlations between inflammatory cytokine levels, cognitive assessments, Aβ1-40, Aβ1-42, Aβ1-42/Aβ levels, and the extent of atrophy in the left hippocampus. These correlations help uncover the associations among these factors and their potential implications for left hippocampal atrophy in *APOE4* carriers. **(D)**.Continuing with *APOE4* carriers, this sub-figure presents the correlations between inflammatory cytokine levels, cognitive assessments, amyloid levels, and the degree of atrophy in the right hippocampus. It provides insights into how these variables are interconnected and their potential influence on right hippocampal atrophy in the *APOE4* carriers.

Supplementary Figure 2| Validation of the effect of *APOE4* on the IL-7R pathway in SY5Y cells. **(A)**.Under fluorescence microscopy, both overexpressing *E3* and *E4* showed very high expression efficiency. **(B)**. *APOE4* reduced the expression levels of *IL7R* and *CD28.*

Supplementary Figure 3| Data Quality Assessment and Visualization of Principal Component Analysis (PCA) Results. **(A)**.This panel provides an assessment of data quality by displaying the content of mitochondrial genes, which is crucial for evaluating the potential impact of mitochondrial gene expression on the analysis. **(B)**.The number of genes detected in the dataset is visualized in this sub-figure, offering insights into the diversity and richness of gene expression in the dataset.

(C).The number of unique molecular identifier (UMI) genes is presented, providing information about the uniqueness and diversity of genes captured in the dataset. **(D)**.The PCA inflection point diagram helps identify the optimal number of principal components to be retained for subsequent analysis, assisting in dimensionality reduction. **(E).** The top 20 principal components, as determined in the previous step, are selected for further clustering analysis, ensuring that the most informative components are used in subsequent analyses.

Supplementary Figure 4| Cell Annotation of PBMC After PCA Dimensionality Reduction and Cell Clustering (Bubble Chart). **(A)**.This panel presents the cell clusters resulting from PCA dimensionality reduction and clustering with a resolution of 1. It offers a visual representation of the identified cell clusters within the PBMC dataset. **(B)**.The distribution of different cell clusters within the experimental groups is depicted, illustrating how various cell populations are distributed among the different groups. **(C)**.Utilizing dataset-specific literature, markers for corresponding cell types, including Macrophages, B cells, NK cells, and T cells, are obtained. Subsequently, corresponding bubble charts are generated to visualize the expression of these markers within the identified cell clusters.

Supplementary Figure 5 | PBMC Clustering and Cell Composition in Relation to *APOE4* Genotype. **(A)**.Annotated clustering of peripheral blood mononuclear cells (PBMCs) provides insights into the distinct cell populations within the samples. **(B)**.Analysis reveals the distribution of different PBMCs between individuals with *APOE4* and non-*APOE4* genotypes. **(C)**.The proportion of each cell type in various groups is graphically presented, highlighting variations in cell composition. **(D)**.Violin plots depict the expression patterns of marker genes, contributing to a comprehensive understanding of the differences in gene expression among various PBMC populations associated with *APOE4* genotype.

Supplementary Figure 6 | Clustering and Analysis of T Cell Subpopulations. **(A)**.T cell subpopulations are annotated based on the results of clustering analysis, allowing for the identification and categorization of distinct T cell clusters. **(B)**.This graph presents the proportion of each T cell cluster within the non-*APOE* carriers group, providing insights into the distribution of T cell subpopulations in individuals without the *APOE* genotype. **(C)**.Similarly, this graph illustrates the proportion of each T cell cluster within the *APOE4* carriers group, revealing the distribution of T cell subpopulations in individuals with the *APOE* genotype. **(D)**.Utilizing dataset-specific literature, we have obtained markers for various T cell subpopulations, including CD4+CD8+ T cells, CD8+ Tem cells, CD8+ naive T cells, CD4+ Treg cells, CD4+ Tem cells, and CD4+ Naive T cells. Corresponding bubble charts have been generated to visualize the expression of these markers within the identified T cell clusters.

Supplementary Figure 7 |Pseudo temporal analysis of CD4 T cell related subpopulations. **(A).** Over time, CD4+ Naïve cells exhibited a progression towards a CD4+ Tem phenotype, eventually culminating in a CD4+ Treg state. (**B**). The trend in the CD4 T cell differentiation remains consistent across both *APOE4* and non-*APOE4* groups. **(C).** Over time, the expression level of IL7R exhibited a gradual increase. **(D).** IL7R expression and CD4+ T cell differentiation remained consistent across both *APOE4* and non-*APOE4* groups.

Supplementary Figure 8| Single-Cell RNA Sequencing Analysis of PBMCs in Alzheimer's Disease Patients with Different *APOE* Genotypes. **(A)**.This sub-figure displays the Uniform Manifold Approximation and Projection (UMAP) visualization of each sample in the study, labeled by cell type annotation using SingleR. It provides a comprehensive view of the cell types identified within the PBMC dataset. **(B)**. An UpSet plot is presented to illustrate the differential expression of genes (DEGs) between individuals with different *APOE* genotypes within each cell type. This plot highlights the unique DEGs associated with various cell populations. **(C)**. A bar chart

showcases the results of Protein-Protein Interaction (PPI) Network Analysis using the Molecular Complex Detection (MCODE) algorithm for the DEGs identified in four different cell types. Notably, the enrichment of the IL-7 signaling pathway is observed among the downregulated genes in T cells, offering insights into the regulatory mechanisms specific to T cell function in relation to *APOE* genotypes.

Supplementary Figure 9| Single-Cell RNA Sequencing Analysis of T Cell Subsets in Alzheimer's Disease Patients. **(A)**.Uniform Manifold Approximation and Projection (UMAP) visualization of T cell subpopulations labeled by cell type annotation. Utilizing SingleR, this analysis identifies four putative cell clusters within the T cell population, shedding light on the heterogeneity of T cell subsets. **(B)**.Protein-Protein Interaction (PPI) Network Analysis reveals the enrichment of the "Cytokine Signaling in Immune System" pathway among the differentially expressed genes (DEGs) between various APOE genotypes within T cell subsets. **(C)**.The IL-7 signaling pathway emerges as enriched within the T cell subsets, particularly within highly connected subnetworks identified using the Molecular Complex Detection (MCODE) algorithm. **(D)**.Cellular communication networks associated with the IL-2 family signaling pathway are presented for non-*APOE4* carriers, offering insights into intercellular signaling patterns within this pathway. **(E).**Similarly, cellular communication networks associated with the IL-2 family signaling pathway are presented for *APOE4* carriers, enabling a comparative analysis of intercellular signaling within this pathway between different *APOE* genotypes.

Supplementary Tables

Supplementary Table-1. Correlation analysis of plasma inflammatory cytokines and hippocampal height

Inflammatory cytokines	Height from HH/HB to TB	Height of HH/HB	Width of Temporal horn

	Pearson's r (95%CI)	*p*-value	Pearson's r (95%CI)	*p*-value	Pearson's r (95%CI)	*p*-value
Left hippocampal head (L-HH)						
TNF-alpha (pg/ml)	0.153 (-0.050 to 0.443)	0.270	0.019 (-0.204 to 0.266)	0.890	0.048 (-0.215 to 0.338)	0.729
IFN-gamma (pg/ml)	-0.035 (-0.213 to 0.229)	0.799	-0.013 (-0.217 to 0.276)	0.928	-0.094 (-0.389 to 0.095)	0.500
IL-1beta (pg/ml)	0.240 (-0.087 to 0.477)	0.280	0.271 (-0.143 to 0.512)	0.048	0.045 (-0.306 to 0.197)	0.747
IL-5 (pg/ml)	0.090 (-0.195 to 0.137)	0.519	-0.049 (-0.437 to 0.213)	0.724	-0.150 (-0.457 to 0.199)	0.451
IL-6 (pg/ml)	0.184 (-0.242 to 0.168)	0.268	0.037 (-0.445 to 0.084)	0.825	0.294 (-0.058 to 0.344)	0.074
IL-7 (pg/ml)	0.298 (0.096 to 0.546)	0.029	0.364 (0.155 to 0.559)	0.007	-0.199 (-0.529 to 0.297)	0.148
IL-8 (pg/ml)	0.148 (-.0414 to 0.313)	0.287	-0.137 (-0.461 to 0.267)	0.323	0.022 (-0.177 to 0.184)	0.875
IL-10 (pg/ml)	0.249 (0.045 to 0.153)	0.069	0.019 (-0.192 to 0.318)	0.432	0.047 (-0.318 to 0.144)	0.734
IL-13 (pg/ml)	0.024 (-0.347 to 0.281)	0.864	0.067 (-0.277 to 0.349)	0.632	-0.007 (-0.385 to 0.343)	0.935
IL-17 (pg/ml)	0.228 (-0.011 to 0.499)	0.097	0.139 (-0.189 to 0.446)	0.316	0.252 (-0.526 to -0.040)	0.066
IL-18 (pg/ml)	0.263 (0.073 to 0.465)	0.056	0.153 (-0.114 to 0.327)	0.270	-0.128 (-0.311 to 0.183)	0.357
IL-33 (pg/ml)	-0.043 (-0.315 to 0.162)	0.757	-0.071 (-0.295 to 0.168)	0.611	0.072 (-0.173 to 0.297)	0.605
MCP-1 (pg/ml)	-0.097 (-0.203 to 0.415)	0.487	-0.089 (-0.206 to 0.385)	0.521	0.159 (-0.128 to 0.458)	0.250

Right hippocampal head (R-HH)						
TNF-alpha (pg/ml)	0.007 (-0.240 to 0.312)	0.960	-0.052 (-0.382 to 0.149)	0.710	0.060 (-0.157 to 0.270)	0.667
IFN-gamma (pg/ml)	-0.156 (-0.410 to 0.125)	0.261	-0.044 (-0.365 to 0.244)	0.752	-0.124 (-0.368 to 0.215)	0.372
IL-1beta (pg/ml)	0.117 (-0.264 to 0.421)	0.400	0.116 (-0.204 to 0.640)	0.444	-0.072 (-0.445 to 0.119)	0.606
IL-5 (pg/ml)	0.051 (-0.284 to 0.353)	0.716	0.002 (-0.251 to 0.284)	0.988	0.040 (-.0400 to 0.284)	0.777
IL-6 (pg/ml)	-0.114 (-0.438 to 0.174)	0.441	-0.139 (-0.556 to 0.116)	0.316	0.190 (0.025 to 0.522)	0.170
IL-7 (pg/ml)	0.205 (-0.040 to 0.438)	0.136	0.253 (0.045 to 0.438)	0.065	0.170 （-0.470 to 0.226）	0.218
IL-8 (pg/ml)	0.024 (-0.109 to 0.354)	0.861	0.029 (-0.102 to 0.192)	0.835	0.202 (-0.252 to 0.483)	0.143
IL-10 (pg/ml)	0.237 (-0.034 to 0.562)	0.084	0.184 (-0.041 to 0.413)	0.182	-0.035 (-0.268 to 0.235)	0.799
IL-13 (pg/ml)	-0.078 (-0.312 to 0.190)	0.574	-0.097 (-0.368 to 0.217)	0.483	0.143 (-0.262 to 0.489)	0.303
IL-17 (pg/ml)	0.103 (-0.208 to 0.453)	0.458	0.111 (-0.339 to 0.510)	0.425	-0.098 (-0.344 to 0.144)	0.479
IL-18 (pg/ml)	0.106 (-0.145 to 0.333)	0.444	0.095 (-0.127 to 0.284)	0.496	0.056 (-0.250 to 0.284)	0.689
IL-33 (pg/ml)	-0.110 (-0.432 to 0.119)	0.428	0.032 (-0.144 to 0.278)	0.818	0.005 (-0.210 to 0.236)	0.971
MCP-1 (pg/ml)	0.130 (-0.210 to 0.423)	0.349	0.125 (-0.150 to 0.415)	0.366	0.123 (-0.115 to 0.480)	0.374
Left hippocampal body (L-HB)						
TNF-alpha (pg/ml)	0.044 (-0.174 to	0.754	0.007 (-0.340 to	0.962	0.161 (-0.203 to	0.246

	0.301)		0.148)		0.457)	
IFN-gamma (pg/ml)	-0.034 (-0.274 to 0.148)	0.086	-0.081 (-0.321 to 0.155)	0.558	-0.131 (-0.368 to 0.124)	0.344
IL-1beta (pg/ml)	0.058 (-0.291 to 0.298)	0.676	-0.020 (-0.280 to 0.186)	0.886	-0.051 (-0.352 to 0.290)	0.714
IL-5 (pg/ml)	0.054 (-0.214 to 0.390)	0.698	-0.016 (-0.282 to 0.213)	0.909	0.170 (-0.418 to 0.194)	0.218
IL-6 (pg/ml)	-0.276 (-0.532 to 0.013)	0.043	-0.148 (-0.467 to 0.169)	0.248	0.249 (0.036 to 0.492)	0.069
IL-7 (pg/ml)	0.289 (0.080 to 0.443)	0.034	0.274 (-0.023 to 0.499)	0.045	-0.180 (-0.504 to 0.245)	0.193
IL-8 (pg/ml)	-0.054 (-0.234 to 0.223)	0.697	-0.028 (-0.251 to 0.255)	0.843	0.173 (-0.260 to 0.383)	0.210
IL-10 (pg/ml)	0.152 (-0.088 to 0.360)	0.271	0.016 (-0.165 to 0.234)	0.907	-0.076 (-0.359 to 0.103)	0.587
IL-13 (pg/ml)	-0.224 (-0.565 to 0.091)	0.103	-0.214 (-0.443 to 0.001)	0.121	-0.092 (-0.358 to 0.153)	0.509
IL-17 (pg/ml)	0.068 (-0.207 to 0.301)	0.218	-0.134 (-0.382 to 0.088)	0.334	-0.245 (-0.416 to 0.013)	0.075
IL-18 (pg/ml)	0.155 (-0.076 to 0.416)	0.264	0.037 (-0.262 to 0.242)	0.793	-0.138 (-0.375 to 0.121)	0.320
IL-33 (pg/ml)	0.032 (-0.165 to 0.329)	0.819	0.028 (-0.256 to 0.249)	0.839	-0.078 (-0.269 to 0.146)	0.573
MCP-1 (pg/ml)	0.119 (-0.279 to 0.232)	0.391	0.104 (-0.141 to 0.277)	0.453	0.112 (-0.085 to 0.248)	0.422
Right hippocampal body (R-HB)						
TNF-alpha (pg/ml)	0.087 (-0.090 to 0.363)	0.531	0.210 (-0.082 to 0.455)	0.182	0.150 (-0.157 to 0.322)	0.451
IFN-gamma (pg/ml)	0.155 (-0.149 to	0.262	0.104 (-0.261 to	0.454	-0.131 (-0.334 to	0.344

	0.467)		0.343)		0.107)	
IL-1beta (pg/ml)	0.117 (-0.396 to 0.375)	0.400	0.106 (-0.114 to 0.361)	0.444	-0.072 (-0.364 to 0.136)	0.606
IL-5 (pg/ml)	0.323 (0.082 to 0.526)	0.017	0.312 (0.066 to 0.567)	0.020	-0.081 (-0.380 to 0.84)	0.559
IL-6 (pg/ml)	-0.104 (-0.371 to 0.244)	0.455	0.134 (-0.210 to 0.483)	0.455	0.298 (0.054 to 0.584)	0.028
IL-7 (pg/ml)	-0.061 (-0.385 to 0.182)	0.661	0.012 (-0.160 to 0.271)	0.933	-0.106 (-0.370 to 0.211)	0.445
IL-8 (pg/ml)	-0.221 (-0.537 to 0.470)	0.108	-0.216 (-0.611 to 0.341)	0.217	-0.001 (-0.229 to 0.147)	0.993
IL-10 (pg/ml)	0.129 (-0.007 to 0.340)	0.351	0.053 (-0.145 to 0.268)	0.704	-0.015 (-0.254 to 0.246)	0.916
IL-13 (pg/ml)	0.058 (-0.206 to 0.389)	0.675	0.082 (-0.136 to 0.403)	0.676	0.162 (-0.086 to 0.436)	0.243
IL-17 (pg/ml)	0.152 (-0.110 to 0.417)	0.273	0.082 (-0.103 to 0.258)	0.556	-0.189 (-0.498 to 0.106)	0.171
IL-18 (pg/ml)	-0.180 (-0.320 to 0.020)	0.194	-0.035 (-0.255 to 0.117)	0.852	0.115 (-0.120 to 0.300)	0.407
IL-33 (pg/ml)	0.108 (-0.175 to 0.426)	0.436	0.198 (-0.066 to 0.450)	0.151	-0.020 (-0.227 to 0.207)	0.888
MCP-1 (pg/ml)	0.016 (-0.191 to 0.099)	0.970	0.134 (-0.173 to 0.381)	0.434	0.199 (-0.137 to 0.403)	0.149

HH:hippocampus head; HB:hippocampus body; TB: bottom of the temporal lobe.

Supplementary Table-2. Correlation analysis of Plasma inflammatory cytokines and plasma β-Amyloid protein

Inflammatory	**Aβ1-42**		**Aβ1-40**		**Aβ1-42/Aβ1-40**	
	Pearson's r	*p*-valu	Pearson's r	*p*-valu	Pearson's r	*p*-valu

cytokines	(95%CI)	e	(95%CI)	e	(95%CI)	e
TNF-alpha (pg/ml)	-0.009 (-0. 330 to 0.180)	0.955	-0.088 (-0.441 to 0.269)	0.597	0.120 (-0.439 to 0.445)	0.474
IFN-gamma (pg/ml)	-0.103 (-0.370 to 0.414)	0.539	-0.015 (-0.546 to 0.392)	0.928	-0.169 (-0.616 to 0.343)	0.310
IL-1beta (pg/ml)	0.003 (-0.321 to 0.152)	0.984	-0.092 (-0.305 to 0.372)	0.581	0.061 (-0.242 to 0.425)	0.716
IL-5 (pg/ml)	-0.116 (-0.268 to 0.393)	0.487	0.042 (-0.445 to 0.404)	0.840	-0.116 (-0.469 to 0.318)	0.489
IL-6 (pg/ml)	0.184 (-0.405 to 0.576)	0.268	0.037 (-0.002 to 0.342)	0.825	0.294 (-0.178 to 0.633)	0.074
IL-7 (pg/ml)	-0.072 (-0.305 to 0.187)	0.665	-0.012 (-0.288 to 0.097)	0.945	-0.056 (-0.315 to 0.135)	0.740
IL-8 (pg/ml)	-0.074 (-0.505 to 0.235)	0.658	-0.111 (-0.328 to 0.321)	0.505	0.004 (-0.270 to 0.362)	0.998
IL-10 (pg/ml)	-0.147 (-0.419 to 0.083)	0.620	-0.83 (-0.445 to 0.248)	0.380	0.072 (-0.270 to 0.380)	0.668
IL-13 (pg/ml)	0.297 (-0.056 to 0.579)	0.055	0.313 (-0.083 to 0.576)	0.070	0.096 (-0.256 to 0.467)	0.568
IL-17 (pg/ml)	-0.064 (-0.462 to 0.226)	0.703	-0.176 (-0.312 to 0.237)	0.291	0.055 (-0.229 to 0.412)	0.742
IL-18 (pg/ml)	0.076 (-0.489 to 0.517)	0.650	-0.090 (-0.416 to 0.548)	0.590	0.105 (-0.422 to 0.571)	0.531
IL-33 (pg/ml)	0.076 (-0.283 to 0.209)	0.652	-0.043 (-0.328 to 0.353)	0.796	0.060 (-0.296 to 0.274)	0.720
MCP-1 (pg/ml)	0.073 (-0.240 to 0.276)	0.665	0.106 (-0.506 to 0.279)	0.526	-0.001 (-0.545 to 0.244)	0.995

Supplementary Figures

Supplementary Figure 1

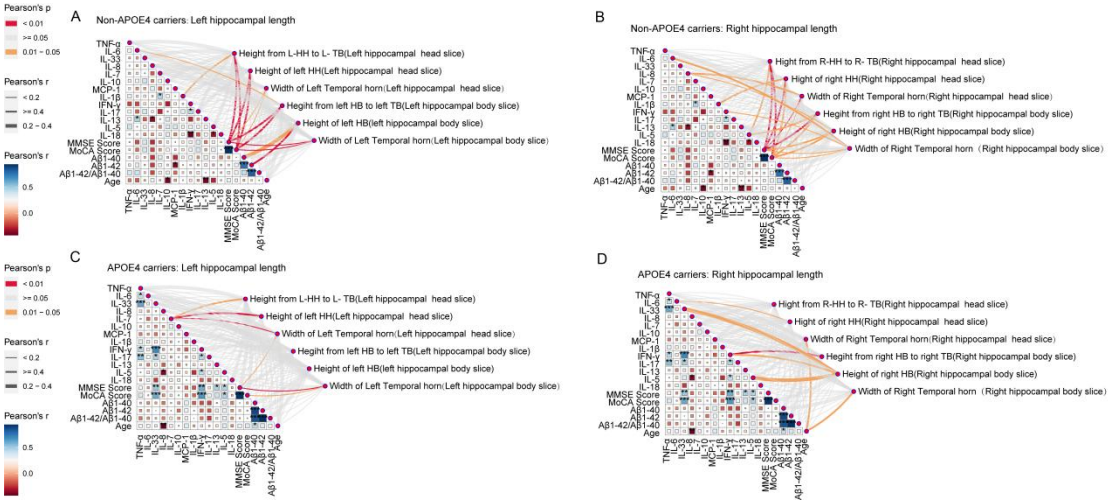

Supplementary Figure 2

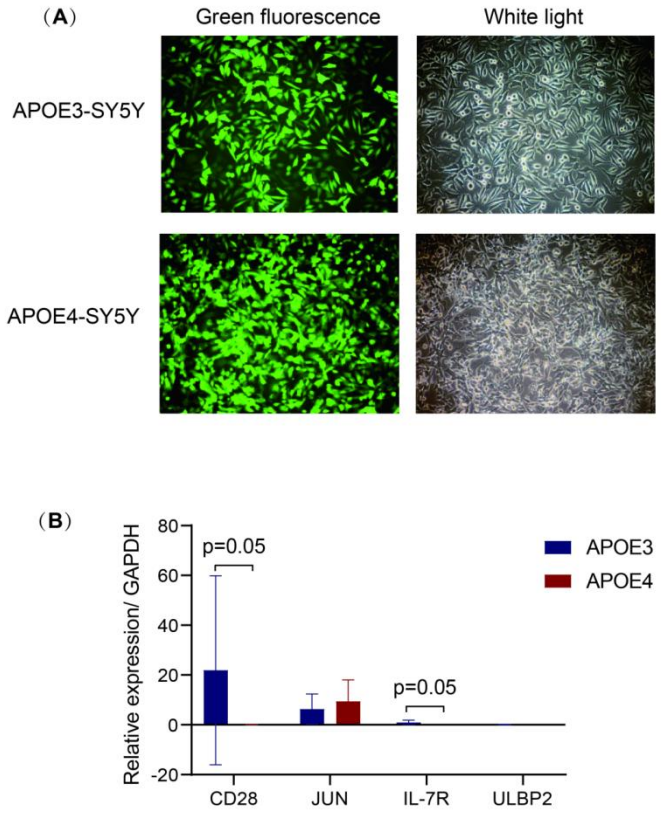

Supplementary Figure 3

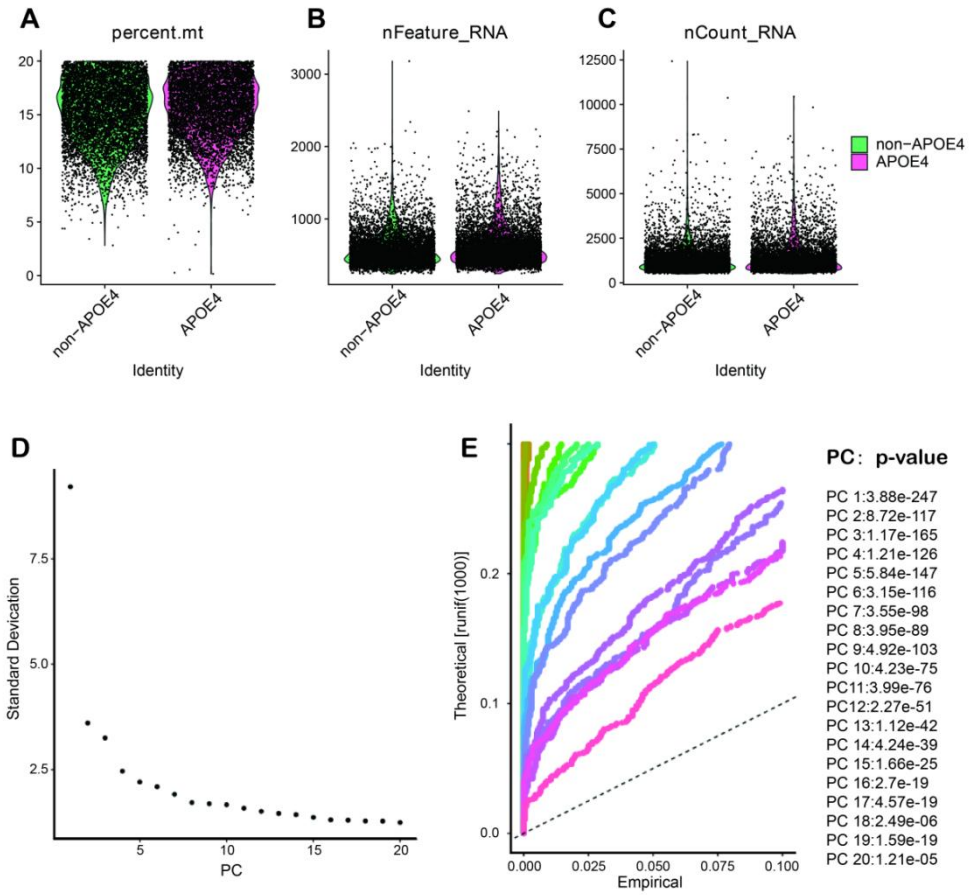

Supplementary Figure 4

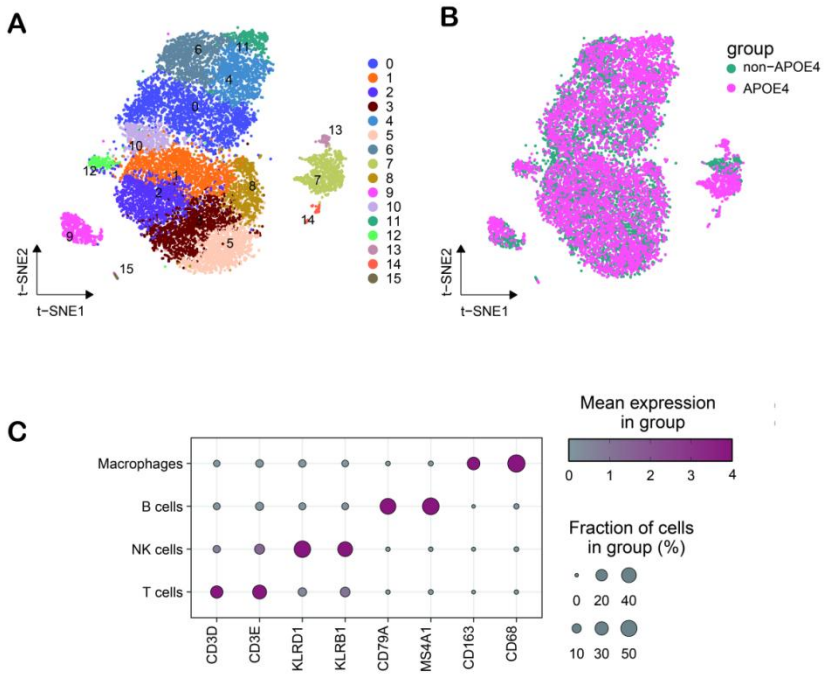

Supplementary Figure 5

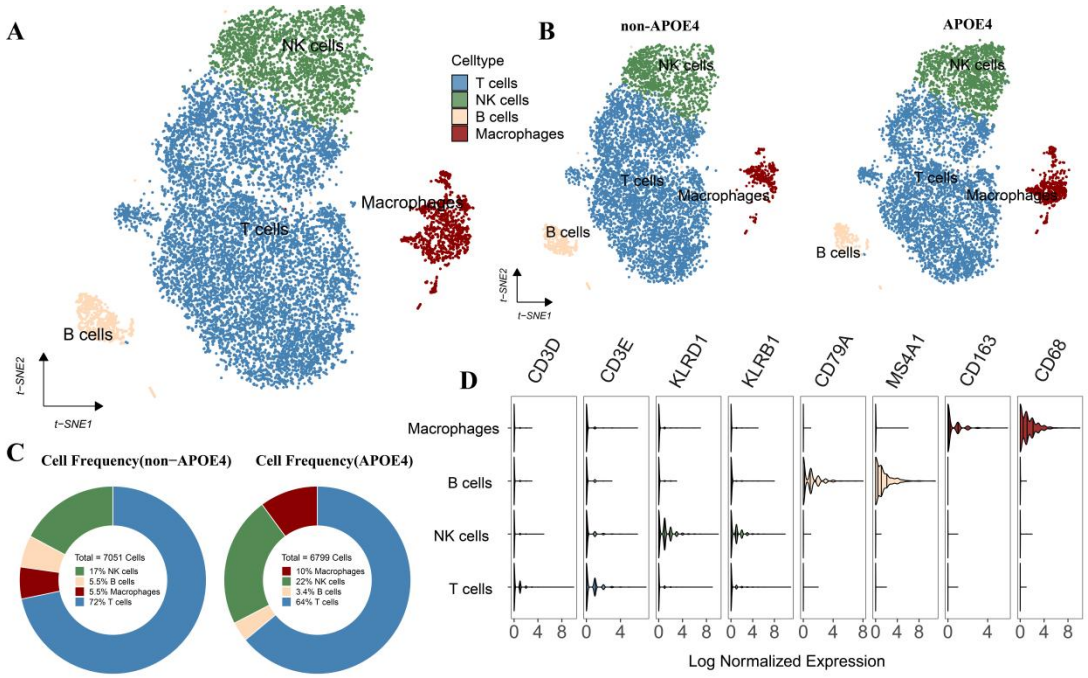

Supplementary Figure 6

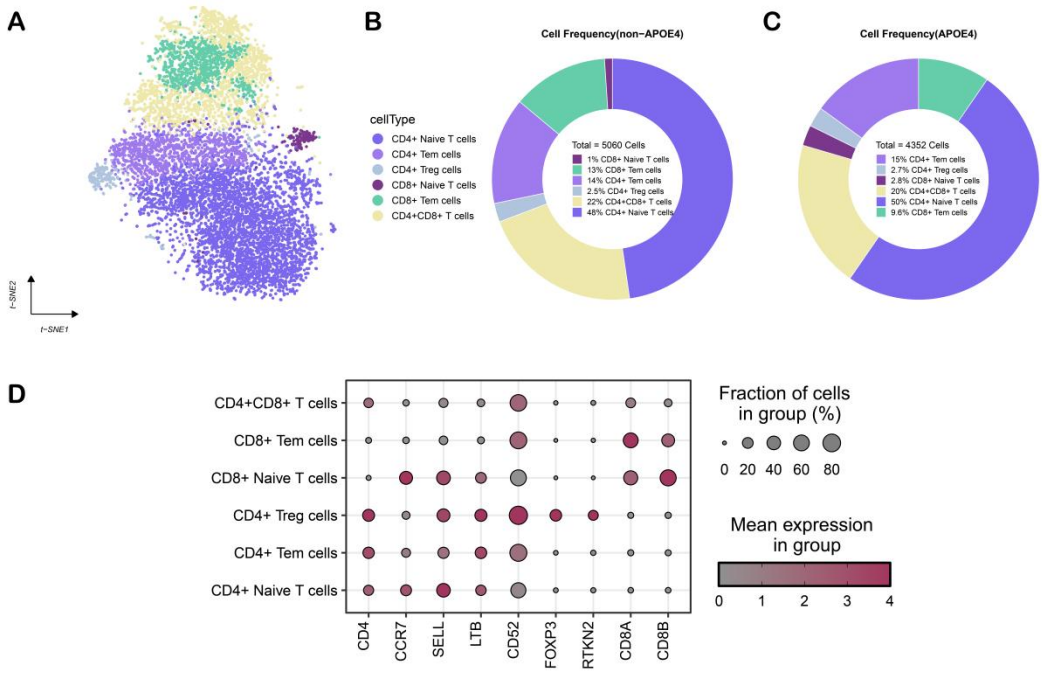

Supplementary Figure 7

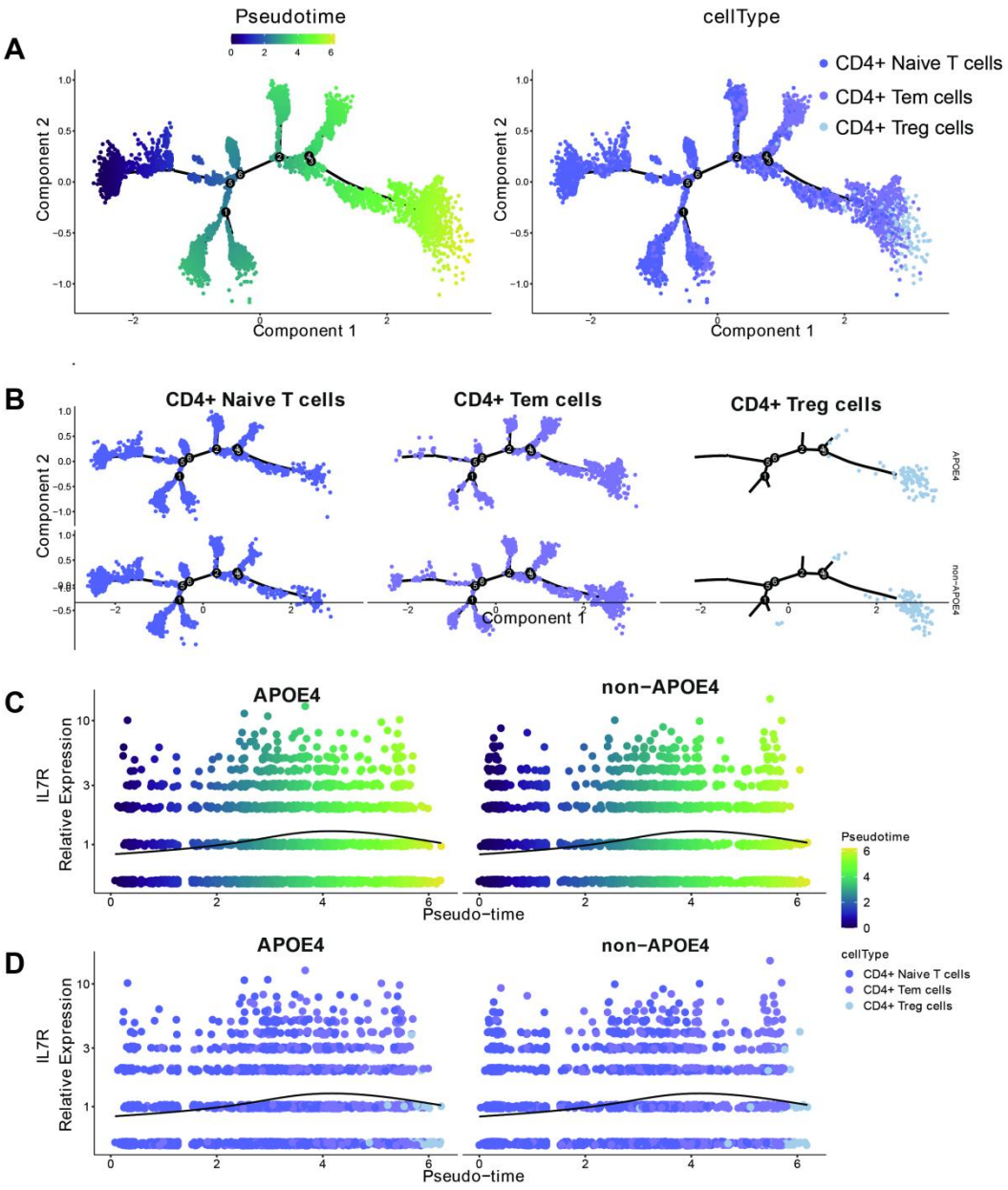

Supplementary Figure 8

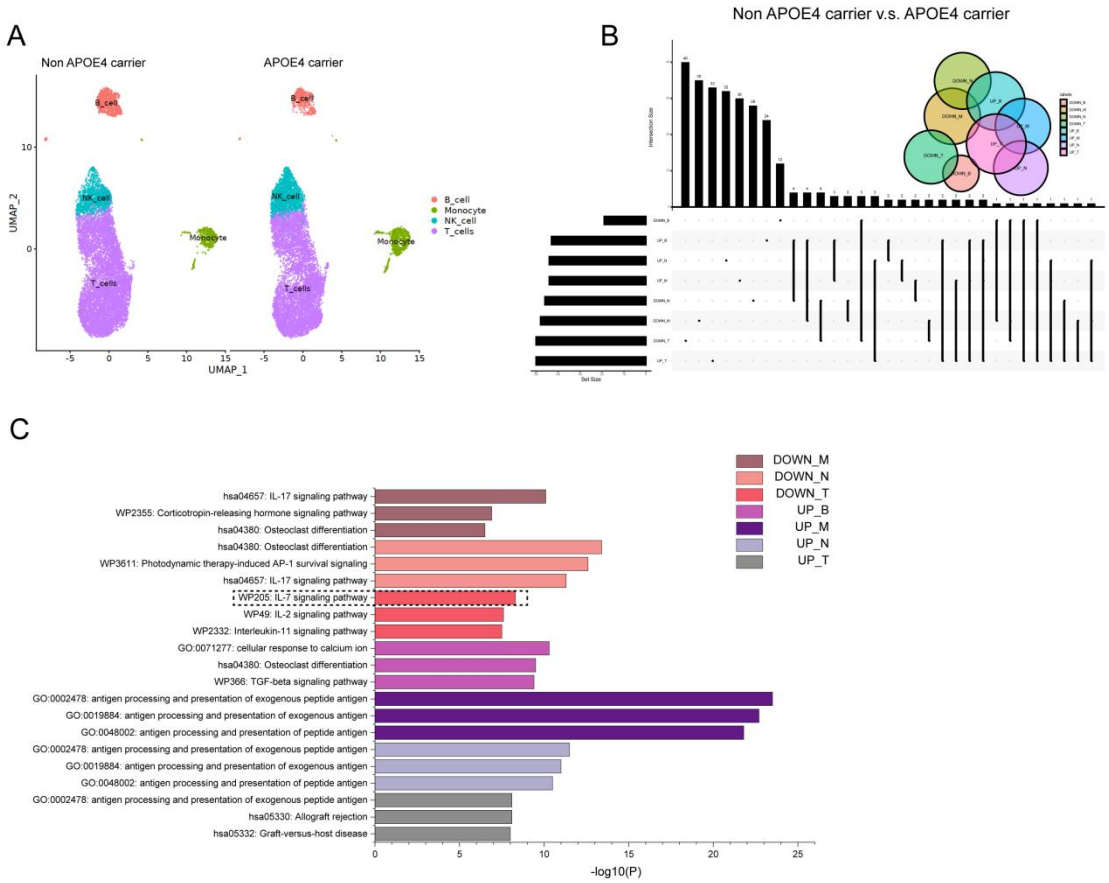

Supplementary Figure 9